

**Revista Mexicana de  
Astronomía y Astrofísica**

Revista Mexicana de Astronomía y Astrofísica

ISSN: 0185-1101

[rmaa@astroscu.unam.mx](mailto:rmaa@astroscu.unam.mx)

Instituto de Astronomía

México

Cho, J.; Lazarian, A.

POLARIZATION OF FIR EMISSION FROM T-TAURI DISKS

Revista Mexicana de Astronomía y Astrofísica, vol. 36, 2009, pp. 155-162

Instituto de Astronomía

Distrito Federal, México

Available in: <http://www.redalyc.org/articulo.oa?id=57115743023>

- How to cite
- Complete issue
- More information about this article
- Journal's homepage in [redalyc.org](http://redalyc.org)

[redalyc.org](http://redalyc.org)

Scientific Information System

Network of Scientific Journals from Latin America, the Caribbean, Spain and Portugal

Non-profit academic project, developed under the open access initiative

## POLARIZATION OF FIR EMISSION FROM T-TAURI DISKS

J. Cho<sup>1</sup> and A. Lazarian<sup>2</sup>

### RESUMEN

Observaciones submilimétricas recientes en 850  $\mu\text{m}$  de discos T-Tauri abren la posibilidad de estudiar la estructura del campo magnético dentro de discos protoestelares. El grado de polarización es de alrededor del 3% y la dirección de ésta es perpendicular al disco. Ya que la emisión térmica de granos de polvo domina la distribución espectral de energía en el submilimétrico e infrarrojo lejano (IRL), se piensa que los granos de polvo son la causa de la polarización. Discutimos el alineamiento del polvo por la radiación y exploramos la eficiencia de alineamiento en discos T-Tauri. Los cálculos muestran que los granos de polvo localizados lejos de la proto-estrella central se alinean con más eficiencia. En la presencia de un campo magnético uniforme los granos alineados emiten radiación polarizada en longitudes de onda del sub-mm/IRL. La dirección de la polarización es perpendicular a la dirección local del campo magnético. Con un modelo reciente de disco T-Tauri y una distribución de granos del tipo Mathis-Rumpl-Nordsieck, con un tamaño máximo de 500–1000  $\mu\text{m}$ , el grado de polarización es de alrededor del 2–3% para longitudes de onda mayores a 100  $\mu\text{m}$ . Nuestro trabajo indica que estudios polarimétricos multi-frecuencia de discos protoestelares pueden ayudar al entendimiento de los detalles de la estructura magnética. También damos predicciones para la emisión polarizada de discos observados en diferentes longitudes de onda y con diferentes ángulos de inclinación.

### ABSTRACT

Recent observations of 850  $\mu\text{m}$  sub-mm polarization from T-Tauri disks open up the possibility of studying the magnetic field structure within protostellar disks. The degree of polarization is around 3% and the direction of polarization is perpendicular to the disk. Since thermal emission from dust grains dominates the spectral energy distribution at sub-mm/far-infrared (FIR) wavelengths, dust grains are thought to be the cause of the polarization. We discuss grain alignment by radiation and we explore the efficiency of dust alignment in T-Tauri disks. The calculations show that dust grains located far away from the central proto-star are more efficiently aligned. In the presence of a regular magnetic field, the aligned grains produce polarized emission in sub-mm/FIR wavelengths. The direction of polarization is perpendicular to the local magnetic field direction. When we use a recent T-Tauri disk model and take a Mathis-Rumpl-Nordsieck-type distribution with maximum grain size of 500–1000  $\mu\text{m}$ , the degree of polarization is around 2–3% level at wavelengths larger than  $\sim 100 \mu\text{m}$ . Our work indicates that multifrequency infrared polarimetric studies of protostellar disks can provide good insights into the details of their magnetic structure. We also provide predictions for polarized emission for disks viewed at different wavelengths and viewing angles.

*Key Words:* accretion, accretion disk — ISM: dust, extinction — polarization — stars: pre-main sequence

### 1. INTRODUCTION

Recently, Tamura et al. (1999) first detected polarized emission from T-Tauri stars, low mass protostars. They interpreted the polarization (at  $\sim 3\%$  level) in terms of thermal emission from aligned dust grains. The magnetic field is an essential component for grain alignment. If grains are aligned with their long axes perpendicular to magnetic field, the resulting grain emission has polarization directed perpendicular to the magnetic field.

The notion that the grains can be aligned in respect to the magnetic field can be traced back to the discovery of star-light polarization arising from interstellar dust grains by Hall (1949) and Hiltner (1949). Historically the theory of the grain alignment was developing mostly to explain the interstellar polarization, but grain alignment is a much wider spread phenomenon (see Lazarian 2007 for a review). Among the alignment mechanisms the one related to radiative torques (RTs) looks the most promising. We invoke it for our calculations below.

The RTs are the result of the interaction of radiation with a grain, and they spin the grain up. The RT alignment was first discussed by Dolginov (1972)

<sup>1</sup>Dept. of Astronomy and Space Science, Chungnam National Univ., Korea (jcho@cnu.ac.kr).

<sup>2</sup>Astronomy Dept., Univ. of Wisconsin, Madison, WI53706, USA (lazarian@astro.wisc.edu).

and Dolginov & Mytrophanov (1976). However, quantitative studies were done only in 1990's. In their pioneering work, Draine & Weingartner (1996, 1997) demonstrated the efficiency of the RT alignment for a few arbitrary chosen irregular grains using numerical simulations. This work identified RTs as potentially the major agent for interstellar grain alignment. A successful analytical model of RTs was suggested by Lazarian & Hoang (2007). Cho & Lazarian (2005) demonstrated a rapid increase of radiative torque efficiency and showed that radiative alignment can naturally explain decrease of the degree of polarization near the centers of pre-stellar cores. Large grains are known to be present in protostellar disk environments and this makes the RT alignment promising.

Roughly speaking, the efficiency of grain alignment by RTs depends on two factors, the intensity of radiation and the gaseous drag. The latter depends on gas pressure. The ideal condition for grain alignment by RTs is strong radiation and low gas pressure.

In order to calculate efficiency of grain alignment in T-Tauri disks, we need to know the intensity of radiation, the gas density, and the temperature. A recently proposed hydrostatic, radiative equilibrium passive disk model (Chiang & Goldreich 1997; Chiang et al. 2001, hereafter C01) fits observed SED from T-Tauri stars very well and seems to be one of the most promising models. Here, passive disk means that active accretion effect, which might be very important in the immediate vicinity of the central star, is not included in the model. Here we adopt the model of C01.

In this paper, we briefly discuss polarized far-infrared (FIR) emission arising from aligned dust grains by radiative torque in T-Tauri disks. Detailed calculations and discussions can be found in Cho & Lazarian (2007). In § 2, we discuss grain alignment in T-Tauri disks. In § 3, we give theoretical estimates for the degree of polarization. In § 4, we discuss observational implications. We give summary in § 5.

## 2. THE DISK MODEL USED FOR THIS STUDY

We assume that the magnetic field is regular and toroidal (i.e. *azimuthal*). We use the T-Tauri disk model of C01. Figure 1 shows schematically the model. The disk is in hydrostatic and radiative equilibrium and shows flaring. They considered a two-layered disk model. Dust grains in the surface layer are heated directly by the radiation from the central star and emit more or less isotropically. One half of the dust thermal emission immediately escapes and

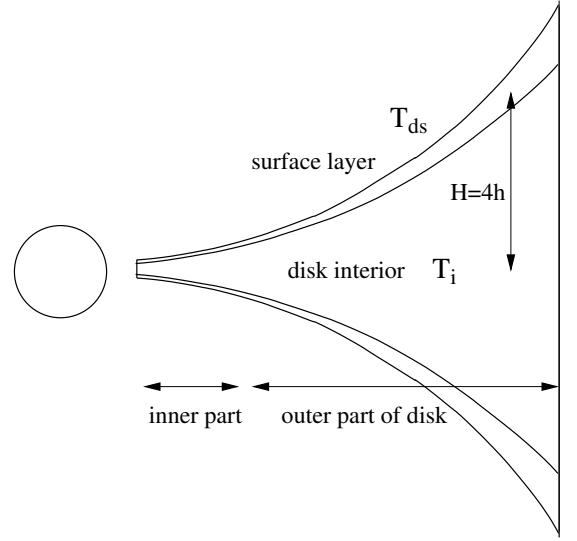
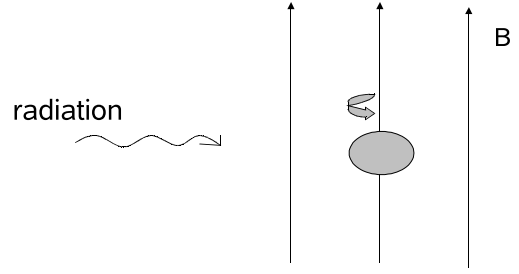
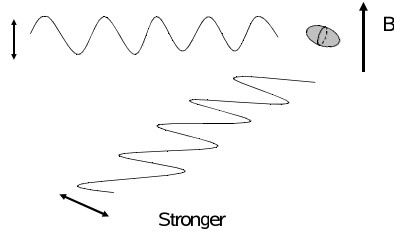


Fig. 1. A schematic view of the disk model (see C01). The surface layer is hotter and heated by the star light. The disk interior is heated by re-processed light from the surface layers. We assume that the disk height,  $H$ , is 4 times the disk scale height,  $h$ . From Cho & Lazarian (2007).

the other half enters into disk interior and heats the dust and gas there. They assume that the disk interior is isothermal.

In our calculations, we use a grain model similar to that in C01. We use a power-law distribution similar to that of Mathis, Rumpl, & Norsieck (1977) for the dust grain sizes; with radii  $a$  between  $a_{\min}$  ( $=0.01 \mu\text{m}$  for both the disk interior and the surface layer),  $a_{\max}$  ( $=1000 \mu\text{m}$  for the disk interior and  $=1 \mu\text{m}$  for the disk surface layer), and with a power index of  $-3.5$ :  $dN \propto a^{-3.5} da$ . As in C01 we assume that the grain composition varies with distance from the central star in both the disk interior and the surface layer. We also assume that the grains in the surface layer are made only of silicate when the distance  $r$  is less than 6 AU, and of silicate covered with water ice when  $r > 6$  AU. We do not use iron grains for the immediate vicinity of the star. We considered that the grains in the disk interior are made of silicate when  $r < 0.8$  AU and ice-silicate for  $r > 0.8$  AU. The fractional thickness of the water ice mantle,  $\Delta a/a$ , is set to 0.4 for both the disk surface and its interior. Unlike C01, we use the refractive index of astronomical silicate (Draine & Lee 1984; Draine 1985; Loar & Draine 1993; see also Weingartner & Draine 2001). We take the optical constants of pure water ice from a NASA web site (<ftp://climate1.gsfc.nasa.gov/wiscombe>).

## Elongated grains emit polarized IR radiation



condition for alignment = fast rotation

Fig. 2. Grain alignment and polarized emission. Left: Emission from an elongated grain. When electric field is parallel to the grain's long axis, the radiation is stronger. Right: Conditions for grain alignment. Roughly speaking, low gas density and strong rotation are favorable conditions for grain alignment.

The column density of the disk is  $\Sigma_0 r_{\text{AU}}^{-3/2}$  with  $\Sigma_0 = 1000 \text{ t g cm}^{-2}$ . Here  $r_{\text{AU}}$  is distance measured in AU. The disk is geometrically flared and the height of the disk surface is set to 4 times the disk scale height  $h$ . The disk inner radius is  $2 R_*$  and the outer radius is 100 AU. The central star has radius of  $R_* = 2.5 R_{\text{Sun}}$  and temperature of  $T_* = 4000 \text{ K}$ . Temperature profile, flaring of disk, and other details of the disk model are described in C01.

## 3. GRAIN ALIGNMENT BY RADIATION

## 3.1. Polarized FIR emission from aligned grains

Theories predict that grain alignment happens in such a manner that the grain's long axis is perpendicular to local magnetic field direction (see Figure 2). Grains are usually cold and emit infrared (IR) radiation. When an elongated grain emits IR radiation it will be stronger when the electric field is parallel to the grain's long axis (see left panel of Figure 2). Thus the direction of polarization is parallel to the grain's long axis, or perpendicular to the magnetic field.

Then, what is the condition of grain alignment? Roughly speaking, fast rotation is a necessary condition for grain alignment. So, what is the condition for fast rotation? Of course, when the intensity of radiation is strong, grains can rotate faster. The gas density is also an important factor. Since gaseous drag slows down grain's rotation, low gas density (more precisely, low gas pressure) is a favorable condition for fast rotation. (Note however that this is just a possible parameterization for RTs. See Lazarian & Hoang 2007 and the last paragraph of this section for details.)

## 3.2. Radiative torque for large grains

For most of the ISM problems, dust grains are usually smaller than the wavelengths of interest.

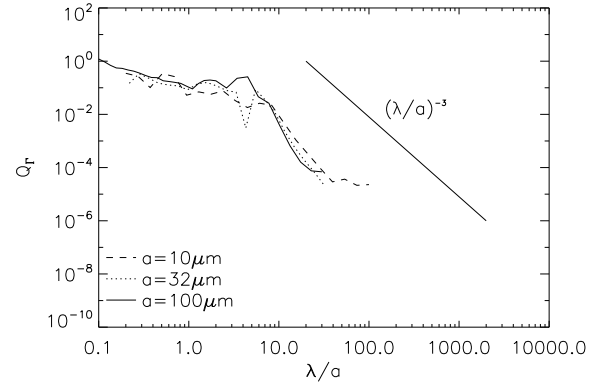


Fig. 3. Behavior of the radiative torque. The torque is  $\sim O(1)$  when  $\lambda \sim a$ , where  $a$  is the grain size. Roughly speaking, torque  $\propto (\lambda/a)^{-3}$ . The results for large grains. Data from Lazarian & Hoang (2007).

However, this is no longer true in T-Tauri disks because we are dealing with grains as large as  $\sim 1000 \mu\text{m}$ . To understand grain alignment in T-Tauri disks we need to know the radiative torque on large grains. Motivated by Figure 3, we assume a radiative torque

$$\Gamma_{\text{rad}} = \pi a^2 u_{\text{rad}} \frac{\lambda}{2\pi} Q_{\Gamma}, \quad (1)$$

with an efficiency factor

$$Q_{\Gamma} = \begin{cases} \sim O(1) & \text{if } \lambda \sim a, \\ \sim (\lambda/a)^{-3} & \text{if } \lambda > a, \end{cases} \quad (2)$$

where  $a$  is the grain size,  $u_{\text{rad}}$  the energy density of the incident radiation, and  $\lambda$  the wavelength of the incident radiation. Note that  $Q_{\Gamma} \sim O(1)$  when  $\lambda \sim a$ .

### 3.3. Rotation rate of dust grains by radiative torque

We assume that to align grains RTs should spin grains suprathermally. Detailed theory of grain alignment can be more complicated (see recent studies by Lazarian & Hoang 2007, 2008; Hoang & Lazarian 2008).

After some modifications, equation (67) in Draine & Weingartner (1996) reads

$$\left(\frac{\omega_{\text{rad}}}{\omega_T}\right)^2 = 4.72 \times 10^9 \frac{\alpha_1}{\delta^2} \rho_3 a_{-5} \left(\frac{u_{\text{rad}}}{n_H kT}\right)^2 \left(\frac{\lambda}{\mu\text{m}}\right)^2 [Q_\Gamma]^2 \left(\frac{\tau_{\text{drag}}}{\tau_{\text{drag,gas}}}\right)^2, \quad (3)$$

where  $Q_\Gamma = \mathbf{Q}_\Gamma \cdot \hat{\mathbf{a}}_1$  and  $\hat{\mathbf{a}}_1$  is the principal axis with largest moment of inertia,  $n_H$  is the hydrogen number density,  $\delta \approx 2$ ,  $\alpha_1 \approx 1.745$ ,  $\rho_3 = \rho/3 \text{ g cm}^{-3}$ ,  $a_{-5} = a/10^{-5} \text{ cm}$ , and  $\omega_T$  is the thermal angular frequency, which is the rate at which the rotational kinetic energy of a grain is equal to  $kT/2$ . The timescales  $\tau_{\text{drag,gas}}$  and  $\tau_{\text{drag,em}}$  are the damping time for gas drag and for electromagnetic emission, respectively, and they satisfy the relation  $\tau_{\text{drag}}^{-1} = \tau_{\text{drag,em}}^{-1} + \tau_{\text{drag,gas}}^{-1}$  (see Draine & Weingartner 1996 for details). As we discussed in the previous subsection,  $Q_\Gamma$  is of order of unity when  $\lambda \sim a$  and declines as  $(\lambda/a)$  increases. From this observation, we can write

$$\begin{aligned} \left(\frac{\omega_{\text{rad}}}{\omega_T}\right)^2 &\approx \left(\frac{\omega_{\text{rad}}}{\omega_T}\right)_{\lambda \sim a}^2 \left(\frac{Q_{\Gamma, \lambda \sim a}}{Q_{\Gamma, \lambda}}\right)^2 \\ &\approx \left(\frac{\omega_{\text{rad}}}{\omega_T}\right)_{\lambda \sim a}^2 \left(\frac{\lambda}{a}\right)^{-6}, \end{aligned} \quad (4)$$

for  $\lambda > a$ , where

$$\begin{aligned} \left(\frac{\omega_{\text{rad}}}{\omega_T}\right)_{\lambda \sim a}^2 &\approx 4.72 \times 10^9 \frac{\alpha_1}{\delta^2} \rho_3 a_{-5} \left(\frac{u_{\text{rad}}}{n_H kT}\right)^2 \\ &\quad \left(\frac{\lambda}{\mu\text{m}}\right)^2 \left(\frac{\tau_{\text{drag}}}{\tau_{\text{drag,gas}}}\right)^2, \end{aligned} \quad (5)$$

The limitation of this approach is that the amplitude values of the RTs are used to parameterize the alignment. In fact, Lazarian & Hoang (2007) showed that the RTs amplitude may change substantially with the angle between the radiation direction and magnetic field.

## 4. GRAIN ALIGNMENT IN DISKS

We use equation (2) to obtain radiative torque ( $Q_\Gamma$ ) on grain particles in the T-Tauri disks. We take a conservative value of  $Q_\Gamma$  at  $\lambda \sim a$ :  $Q_\Gamma \sim 0.1$  at  $\lambda \sim$

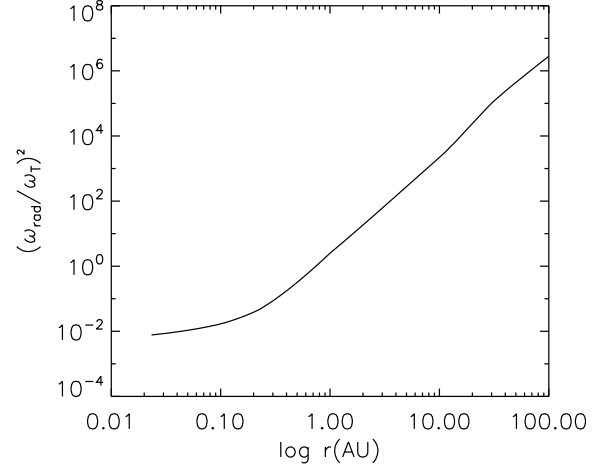


Fig. 4. Grain alignment in the surface layer. The ratio  $(\omega_{\text{rad}}/\omega_T)_{\lambda \sim a}^2$  exceeds 10 when  $r \geq 1 \text{ AU}$ , which means that some grains in the surface layer are aligned when  $r \geq 1 \text{ AU}$ . Results are for  $a = 1 \mu\text{m}$  grains. From Cho & Lazarian (2007).

*a.* Apart from  $Q_\Gamma$ , we also need to know  $u_{\text{rad}}$  and  $n_H$  to get the  $(\omega_{\text{rad}}/\omega_T)_{\lambda \sim a}^2$  ratio (see equation 5). We directly calculate  $u_{\text{rad}}$  and  $n_H$  using the disk model in C01. We assume that  $\tau_{\text{drag}} \sim \tau_{\text{drag,gas}}$ , and that the RT alignment is perfect<sup>3</sup> when the ratio  $(\omega_{\text{rad}}/\omega_T)_{\lambda \sim a}^2$  exceeds a value of 10. Calculations (see Cho & Lazarian 2007) show that grains near the central star cannot be aligned due to the high gas density (high gaseous drag) near the star. Figure 4 shows how the ratio  $(\omega_{\text{rad}}/\omega_T)_{\lambda \sim a}^2$  exceeds 10 when the distance from the central star,  $r$ , is large, which means that grains in the surface layer are aligned when  $r$  is large. We expect that polarized emission from the surface layer is originated from outer part of the disk. Similar results hold true for disk interior. Calculations show that, at large  $r$ , large grains are aligned even deep inside the interior. On the other hand, at small  $r$ , only grains near the disk surface are aligned (see an illustration in Figure 5).

## 5. PREDICTIONS FOR DEGREE OF POLARIZATION

### 5.1. Estimates for Spectral Energy Distribution

We calculate the degree of polarization of emitted infrared radiation from a disk with structure and parameters as described in C01. In this subsection, we assume that the disk is face-on. The degree of polarization will be zero for a face-on disk when magnetic

<sup>3</sup>The perfect alignment is true for grains having superparamagnetic inclusions (Lazarian & Hoang 2008). For ordinary paramagnetic grains the degree of alignment can vary.

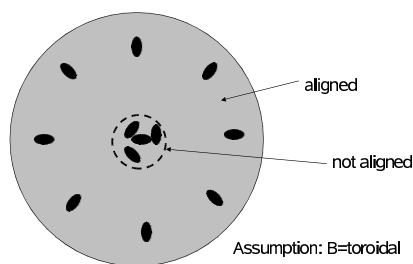


Illustration of alignment (for  $1\mu\text{m}$  grains on surface)

Fig. 5. Illustration of grain alignment on disk surface. Near the star, grains are not aligned due to the high density (high gaseous drag).

field is perfectly azimuthal and the disk is cylindrically symmetric. In this section, *we are concerned only with the absolute magnitude of the polarization*.

Figure 6 shows the results for 1.3:1 oblate spheroid. The degree of polarization can be as large as  $\sim 5\%$  in the FIR/sub-millimeter wavelengths and  $\sim 10\%$  at the mid-IR. The polarized emission at FIR is dominated by the disk interior and that at mid-IR is dominated by the disk surface layer. Note again that, in these calculations, we ignored the direction of polarization and we only take the absolute value of it. Note that, since the degree of polarization of emission from the disk surface layer is very sensitive to the maximum grain size in the surface layer, the results for  $\lambda < 100\mu\text{m}$  should be very sensitive to the maximum grain size in the surface layer.

### 5.2. Radial energy distribution

Figure 7 shows the radial distribution of the emitted radiation. For  $\lambda = 850\mu\text{m}$ , the radiation emitted from both the disk interior and the surface layer are dominated by the outer part of the disk. But, for  $\lambda = 10\mu\text{m}$ , the inner part of the disk contributes with a significant portion of the polarized emission and of the total emission.

### 5.3. Effects of disk inclination

In this subsection we calculate actual degree of polarization that we can observe. Chiang & Goldreich (1999) calculated spectral energy distribution (SED) from inclined disks. We follow a similar method to calculate the SED of polarized emission.

Figure 8 shows the effects of the disk inclination. We calculate the polarized emission from the disk interior. The viewing angle  $\theta$  (= the angle of disk inclination) is the angle between the disk symmetry axis and the line of sight. We plot the direction of

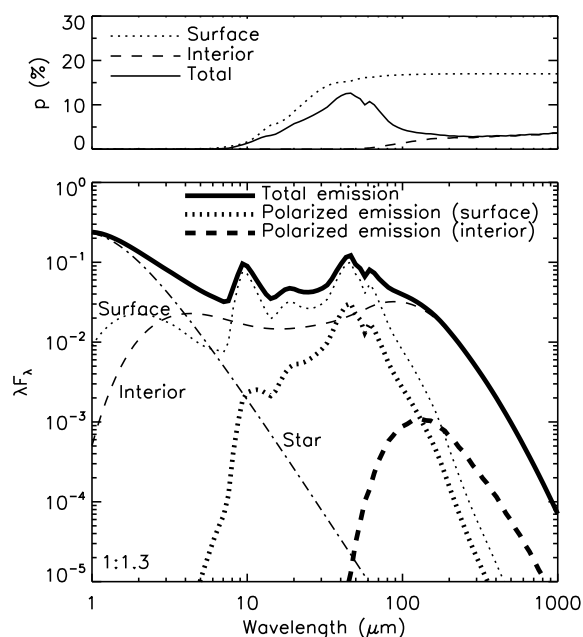


Fig. 6. Top: Degree of polarization of the emission from the surface, the interior, as well as the total emission (dotted, dashed, and solid lines, respectively). Bottom: spectral energy distribution, the vertical axis (i.e.  $\lambda F_\lambda$ ) is in arbitrary units. Thick solid line: total (i.e. interior + surface) emission from disk. Thin dotted line: total emission from disk surface. Thick dotted line: polarized emission from disk surface. Thin dashed line: total emission from disk interior. Thick dashed line: polarized emission from disk interior. Note that, in these calculations of polarized emission, we ignored the direction of polarization vectors and we only take the absolute value of them. The results are for oblate spheroid grains with an axis ratio of 1.3:1. From Cho & Lazarian (2007).

polarization for 3 different wavelengths and 2 different viewing angles. The lines represent the direction of polarization. Since we assume that magnetic field is azimuthal, the direction of polarization is predominantly radial (see lower panels).

## 6. PROSPECTS

Multifrequency observations of protostellar disks have become a booming field recently. As dust grains at different optical depths have different temperatures, multifrequency measurements reveal the structure of the disk. They have advanced substantially our knowledge of the disks and allowed theoretical expectations to be tested.

Our study reveals that multifrequency polarimetry is very important for the protostellar disks. The synthetic observations that we provide explicitly show that observations at wavelength less than

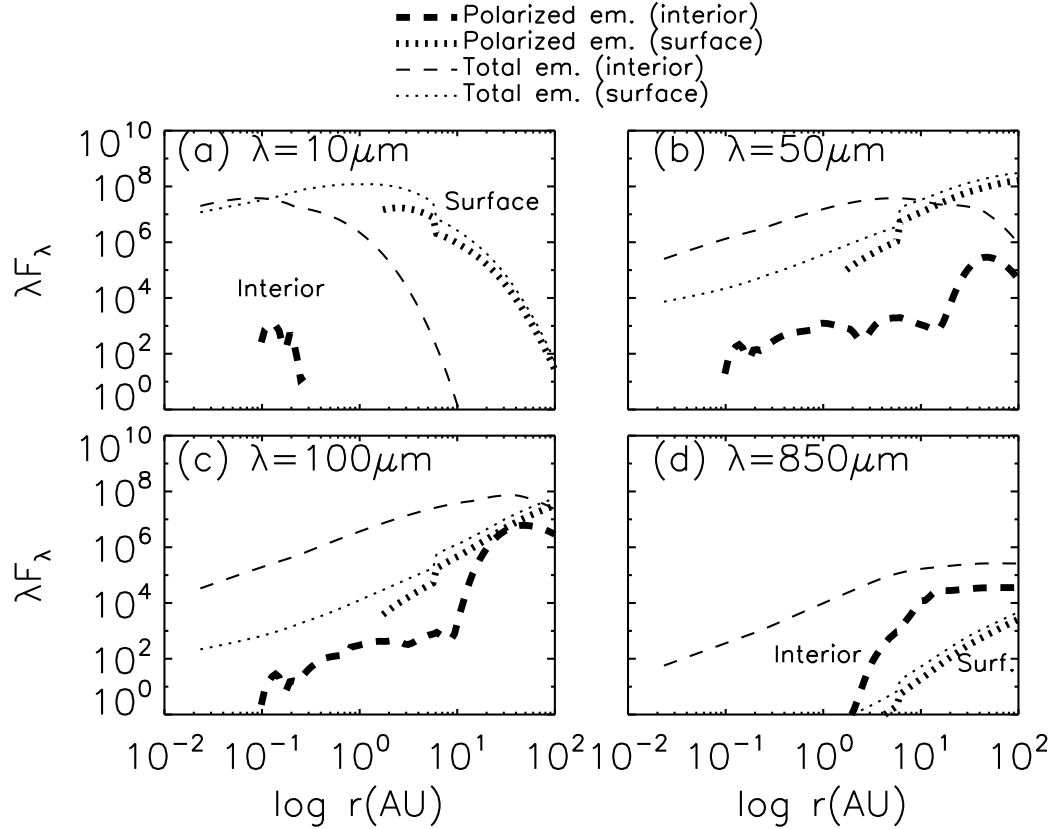


Fig. 7. Radial energy distribution. (a)  $\lambda = 10 \mu\text{m}$ . The inner part of the disk emits substantial amount of radiation. But it emits negligible amount of polarized radiation. Note that, when  $r < 1$  AU, the grains in the surface layer are not aligned and only a negligible fraction of the grains are aligned in the interior (see Figure 4 for disk surface). (b)  $\lambda = 50 \mu\text{m}$ . (c)  $\lambda = 100 \mu\text{m}$ . (d)  $\lambda = 850 \mu\text{m}$ . The result for  $\lambda = 450 \mu\text{m}$  (not shown) is very similar to that for  $\lambda = 850 \mu\text{m}$ . From Cho & Lazarian (2007).

$100 \mu\text{m}$  mostly probe the magnetic fields of the skin layers, while at longer wavelengths they probe the magnetic fields of the bulk of the disk. Therefore polarimetry can, for instance, test models of accretion, e.g. layered accretion (Gammie 1996). Combining the far-infrared polarimetry with polarimetric measurements at different frequencies may provide additional insight into the magnetic properties of protostellar accretion disks.

Most of the present day polarimetry will be done for not resolved protostellar disks. The size of the T-Tauri disks is usually less than  $\sim 300$  AU (see, for example, C01). If we take the distance to proto-stars to be around  $\geq 100$  pc, then the angular sizes of the disks are usually smaller than  $6''$ . The angular resolution of SCUBA polarimeter (SCUPOL) is around  $14''$  (Greaves et al. 2000) and that of SHARC II polarimeter (SHARP; Novak et al. 2004) at  $350 \mu\text{m}$  is around  $9''$ . Therefore it is not easy with currently

available instruments to obtain plots like those of Figure 8. However, the angular resolution of the intended polarimeter on SOFIA will be around  $5''$  at  $53 \mu\text{m}$ ,  $9''$  at  $88 \mu\text{m}$ , and  $22''$  at  $215 \mu\text{m}$ . Thus the intended SOFIA polarimeter will be at the edge of resolving structure of close-by disks, while other instruments will not resolve a typical T-Tauri disk. Therefore for most of the near future observations our predictions in Figures 6 and 8 are most relevant.

## 7. SUMMARY

Making use of the recent advances in grain alignment theory we calculated grain alignment by RTs in a magnetized T-Tauri disk. Based on this, we calculated the polarized emission from the disk. Our results show that

- The polarization arising from aligned grains reveals magnetic fields of T-Tauri disks.
- The disk interior dominates the polarized emission in FIR/sub-millimeter wavelengths.

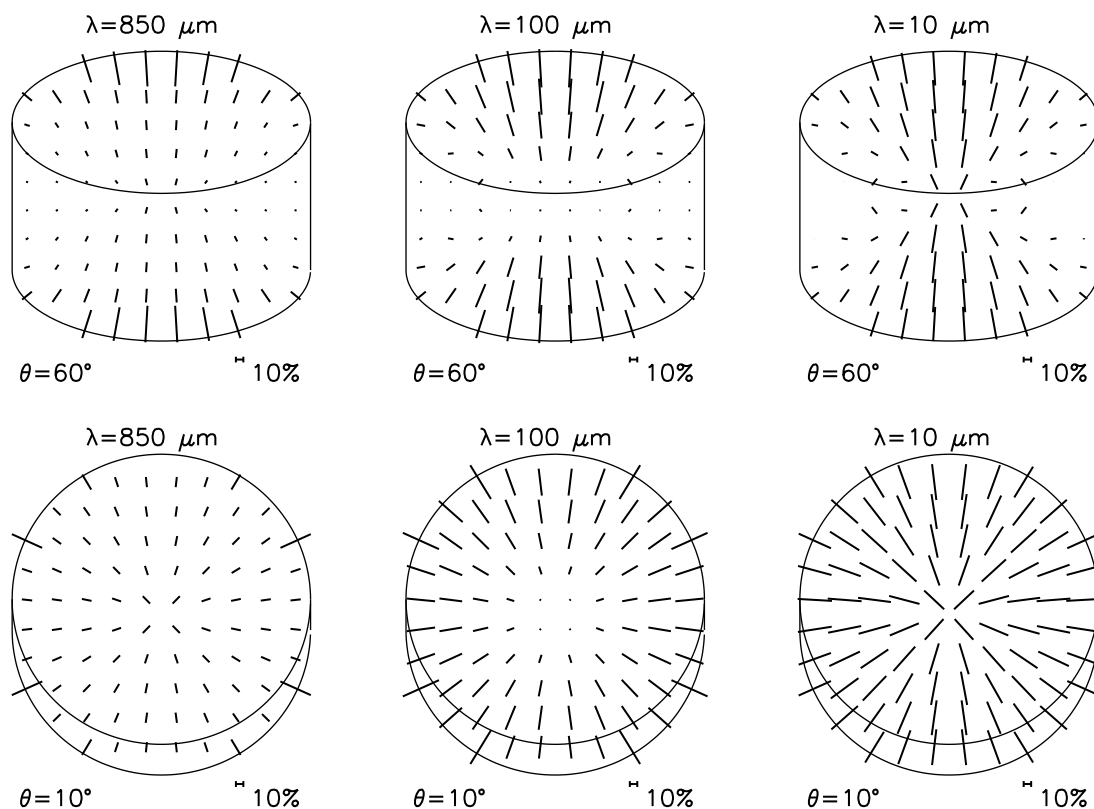


Fig. 8. Simulated observations. The degree of polarization is calculated for the total radiation (i.e. interior + surface) from the disk. The disk inclination angle  $\theta$  is the angle between disk symmetry axis and the line of sight. From Cho & Lazarian (2007).

- The disk surface layer dominates the polarized emission in mid-IR wavelengths. The degree of polarization is very sensitive to the maximum size of grain in the disk surface layer.

- Our study of the effect of the disk inclination predicts substantial changes of the degree of polarization with the viewing angle. The upcoming mid-IR/FIR polarimeters are very promising for studies of magnetic fields in protostellar disks.

- Polarization at different wavelengths reveals aligned grains at different optical depths, which allows one to make a tomography of magnetic field structure.

Jungyeon Cho's work was supported by Korea Foundation for International Cooperation of Science & Technology (KICOS) through the Cavendish-KAIST Research Cooperation Center. A. Lazarian acknowledges the support by the NSF grants AST 02 43156 and AST 0507164, as well as by the NSF Center for Magnetic Self-Organization in Laboratory and Astrophysical Plasmas.

## REFERENCES

- Chiang, E., & Goldreich, P. 1997, *ApJ*, 490, 368  
 ———. 1999, *ApJ*, 519, 279  
 Chiang, E., Joungh, M., Creech-Eakman, M., Qi, C., Kessler, J., Blake, G., & van Dishoeck, E. 2001, *ApJ*, 547, 1077 (C01)  
 Cho, J., & Lazarian, A. 2005, *ApJ*, 631, 361  
 ———. 2007, *ApJ*, 669, 1085  
 Davis, L., & Greenstein, J. L. 1951, *ApJ*, 114, 206  
 Dolginov, A. Z. 1972, *Ap&SS*, 16, 337  
 Dolginov, A. Z., & Mytrophanov, I. G. 1976, *Ap&SS*, 43, 291  
 Draine, B. 1985, *ApJS*, 57, 587  
 Draine, B., & Flatau, P. 1994, *J. Opt. Soc. Am. A*, 11, 1491  
 Draine, B., & Lee, H. 1984, *ApJ*, 285, 89  
 Draine, B., & Weingartner, J. 1996, *ApJ*, 470, 551  
 ———. 1997, *ApJ*, 480, 633  
 Gammie, C. 1996, *ApJ*, 462, 725  
 Greaves, J., Holland, W., Jenness, T., & Hawarden, T. 2000, *Nature*, 404, 732  
 Hall, J. 1949, *Science*, 109, 166  
 Hiltner, W. 1949, *Science*, 109, 165

- Hoang, T., & Lazarian, A. 2008, MNRAS, 388, 117
- Laor, A., & Draine, B. 1993, ApJ, 402, 441
- Lazarian, A. 2007, J. Quant. Spectrosc. Rad. Transfer, 106, 225
- Lazarian, A., & Hoang, T. 2007, MNRAS, 378, 910
- \_\_\_\_\_. 2008, ApJ, 676, 25
- Mathis, J., Rumpl, W., & Nordsieck, K. 1977, ApJ, 217, 425
- Novak, G., et al. 2004, Proc. SPIE, 5498, 278
- Purcell, E. 1979, ApJ, 231, 404
- Tamura, M., Hough, J., Greaves, J., Morino, J.-I., Chrysostomou, A., Holland, W., & Momose, M. 1999, ApJ, 525, 832
- Weingartner, J., & Draine, B. 2001, ApJ, 548, 296